PROCEEDINGS, Twentieth Workshop on Geothermal Reservoir Engineering
Stanford University, Stanford, California, January 24-26 1995
SGP-TR-150

CHEMICAL WATER/ROCK INTERACTION UNDER RESERVOIR CONDITION

K. Watanabe[1], K. Tanifuji[1], H. Takahashi[1],
Y. Wang[2], N. Yamasaki[3] and K. Nakatsuka[2]

1 Research Institute for Fracture Technology, Faculty of Engineering, Tohoku Univ., Sendai 980, JAPAN
2 Department of Resources Engineering, Faculty of Engineering, Tohoku Univ., Sendai 980, JAPAN
3 The Research Laboratory of Hydrothermal Chemistry, Faculty of Science, Kochi Univ., Kochi 780, JAPAN

ABSTRACT

A simple model is proposed for water/rock interaction in rock fractures through which geothermal water flows. Water/rock interaction experiments were carried out at high temperature and pressure (200~350 °C, 18 MPa) in order to obtain basic solubility and reaction rate data. Based on the experimental data, changes of idealized fracture apertures with time are calculated numerically. The results of the calculations show that the precipitation from water can lead to plugging of the fractures under certain conditions. Finally, the results are compared with the experimental data.

INTRODUCTION

Recently geothermal energy extraction from the crust via Hot Dry Rock (HDR) (Tester, 1989; Robinson and Pendergrass, 1989) or Hot Wet Rock (HWR) (Takahashi and Hashida, 1992) systems have received much attention. Thermal energy is extracted by circulating water through artificial and/or natural underground fracture networks.

Because the fractures in such systems are filled with geothermal water, it is necessary to examine the effect of chemical interaction between water and rock on water circulation. Water temperature and its change through the flow path is one of the most important variables for chemical interactions such as dissolution and precipitation. Few published sources are available for rock dissolution. Hashida and Takahashi (1983) performed dissolution experiments using granite. On the other hand, there are many report about the dissolution behavior of quartz, one of commonest rock forming minerals (Kennedy, 1950; Kitahara, 1960; Rimsted et al., 1980). They show that the solubility of quartz has a maximum value at around 320 °C, and thereafter decreases with increasing temperature.

In this paper, a simple model of water/rock interaction in a one-dimensional fracture is developed. In order to obtain the basic parameters for this model, granite dissolution experiments at high temperatures and high pressure are performed with batch and one-through autoclaves. The solubility of granite at several temperatures is obtained from the batch autoclave experiment, and the reaction rates are obtained from the one-through autoclave experiment. The influence of temperature on water/rock interaction is discussed. Based on the experimental results, the changes of fracture aperture caused by rock dissolution and precipitation are modeled numerically. Finally, these numerical results are compared with the experimental results from a tube-reactor autoclave which is constructed to simulate water flow in rock fractures.

WATER/ROCK INTERACTION MODEL

Chemical interactions between rock and water have not yet been fully described, and therefore, there is no well established set of equations which describe rock/water interactions. In this paper we assumed that the rock dissolution can be expressed by following equation :

$$\frac{\partial C}{\partial t} = \frac{S}{M} \cdot K(T) \cdot \{C^{\infty}(T) - C\} \qquad (1)$$

where C is concentration of rock and t is time. M is amount of water involved in the reaction, and S is the water/rock contact area. K is the dissolution rate constant and C^{∞} is the solubility of rock, and both values are functions of temperature, T. Equation 1 is the key equation for the water/rock interaction model presented in this paper.

Although the apertures of natural fractures are unlikely to be spatially uniform, we assume that water flow can be approximated by that in a parallel-sided fracture with a uniform aperture as shown in Fig. 1.

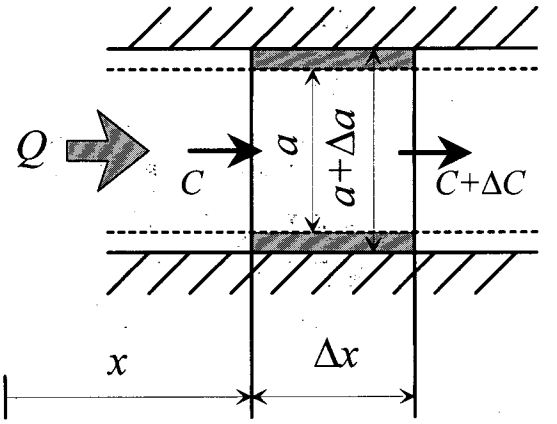

Fig. 1 The model of rock dissolution in a fracture.

Consider a small length, Δx at the point x at time t, with fracture aperture $a(x,t)$ as shown in Fig. 1, the mass balance of water/rock interaction is expressed as :

$$\rho_R \cdot \Delta x \cdot \Delta a(x,t) = \Delta C(x,t) \cdot \rho_W \cdot Q \cdot \Delta t \qquad (2)$$

where ρ_R and ρ_W are the densities of rock and water. Q is water flux through the fracture. Letting $\Delta t \rightarrow 0$ and $\Delta x \rightarrow 0$, equation 2 can be transformed to the following equation which expresses the rate of the aperture change along the fracture.

$$\frac{\partial a(x,t)}{\partial t} = \frac{\rho_W \cdot Q}{\rho_R} \cdot \frac{\partial C(x,t)}{\partial x} \qquad (3)$$

Considering the temperature at this point as $T(x,t)$, according to equation 1, the change of concentration, $\Delta C(x,t)$ is calculated as :

$$\Delta C(x,t) = \frac{2 \cdot \Delta x}{\rho_W \cdot Q \cdot \Delta t} \cdot K(T(x,t)) \cdot \left\{C^{\infty}(T(x,t)) - C(x,t)\right\} \cdot \Delta t \qquad (4)$$

Letting $\Delta x \rightarrow 0$, equation 4 can be transformed to the following equation which express the concentration along the fracture.

$$\frac{\partial C(x,t)}{\partial x} = \frac{2}{\rho_W \cdot Q} \cdot K(T(x,t)) \cdot \left\{C^{\infty}(T(x,t)) - C(x,t)\right\} \qquad (5)$$

Combining equations 3 and 5 :

$$\frac{\partial a(x,t)}{\partial t} = \frac{2}{\rho_R} \cdot K(T(x,t)) \cdot \left\{C^{\infty}(T(x,t)) - C(x,t)\right\} \qquad (6)$$

Equation 6 expresses the rate of fracture aperture change with time, and the fracture aperture at any position and any time can be calculated using this equation. However, in order to use equation 6 in numerical analysis, the solubility, C^{∞} and the dissolution rate constant, K have to be measured as functions of temperature.

THE SOLUBILITY OF GRANITE

The reaction processes between water and granite are very complicated due to its composition. It is therefore impossible to determine a solubility for granite sensuo stricto. Therefore the "apparent solubility" has been assumed to be the solubility of granite, as explained in following discussion.

The granite used in this study comes from Fukusima, Japan, and the mineral composition is shown in Table 1.

Mineral	Quartz	Orthoclase	Albite	Anorthosite	Biotite
Formula	SiO2	KAlSi3O8	NaAlSi3O8	CaAl2Si2O8	Omission
Vol. %	37 %	23 %	24 %	10 %	6 %

Table 1. Mineral composition of Fukushima granite.

Specimens are cut into small plates whose sizes are 45 mm x 40 mm x 5 mm, polished by 1500 mesh sand paper, and washed in acetone to remove cutter oil. Fig. 2 illustrates the batch type autoclave and specimen holder. This autoclave can be operated at temperatures up to 350 °C and pressures up to 20 MPa.

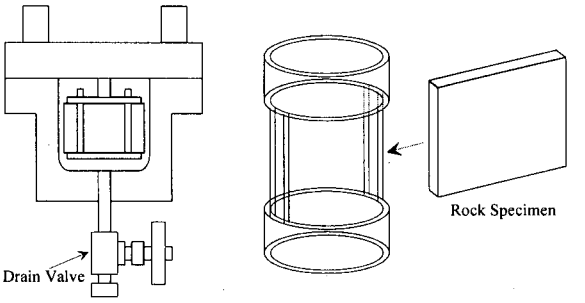

Fig. 2 Batch autoclave. Rock specimens are fixed by the specimen holder, and located in the middle of the autoclave.

Experiments were carried for several run times at temperatures of 200 °C, 250 °C, 300 °C, 330 °C and 350 °C, at a pressure of 18 MPa. After each run, the reacted water was extracted through the drain valve without cooling the autoclave. The specimens were weighed before and after the experiment to calculate the weight loss. In this study, the "granite" concentration in the reacted water was determined from the weight loss of specimens, not from solution analysis.

Figure 3 shows the relationship between time and weight loss expressed as a concentration in the fluid for each temperature.

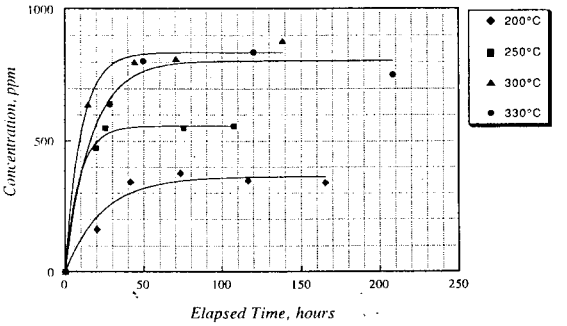

Fig. 3 The weight loss with time caused by dissolution.

Due to precipitation on the inside of autoclave, it was impossible to measure the concentration for the experiments at 350 °C. The results for 350 °C are not shown in Fig. 3. Because the saturated vapor pressure of water at 350 °C is close to 18 MPa, and the precipitation occurred in an air layer, the precipitation may have caused by boiling of the water.

As mentioned before, the strict solubility of granite can not be determined because it is almost impossible to know all the reactions between water and rock. In this paper,

however, we introduce apparent solubility as a tentative solubility for granite. We have already assumed that the interaction between water and rock was governed by equation 1. Integrating equation 1 with time, t, and appling the condition, C=0 when t=0, the equation to express the relationship between the run time and the concentration is obtained as follows for these experiments.

$$C(t) = C^{\infty}(T) \cdot \left\{ 1 - \exp\left(-\frac{S}{\rho_W \cdot V} \cdot K(T) \cdot t \right) \right\} \qquad (7)$$

In equation 7, S is the total reaction interface which is assumed to be equal to geometrical surface area in this study, and V is the volume of water in the autoclave. The unknown values in equation 7 are $C^{\infty}(T)$ and $K(T)$. By fitting equation 7 to the experimental results using a least squares method, both the "apparent solubility", $C^{\infty}(T)$ and the dissolution rate constant, $K(T)$ have been determined in this study. Each fitting curve is shown in Fig. 3. The "apparent solubility" is defined as the solubility of granite in this study. Fig. 4 shows the solubility of granite for each temperature obtained from these experiments. The solubility of quartz measured by Kennedy (1950) and Kitahara (1960) are also shown in Fig. 4.

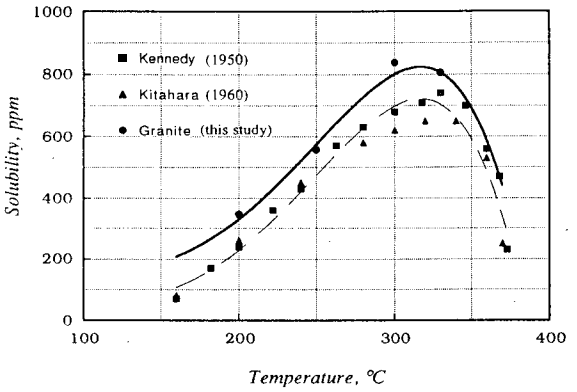

Fig. 4 The "granite" solubility as a function of temperature. The solid curve is used for numerical analysis. The solubility of quartz is also shown.

Although the dissolution rate constants, $K(T)$, for each temperature was measured by these experiments, these values may have large errors caused during heat up time of the autoclave. We, therefore, performed another set of experiments to measure $K(T)$ using the one-through autoclave as discussed next session.

THE DISSOLUTION RATE CONSTANT FOR GRANITE

Granite dissolution experiments in circulating water were performed using one-through autoclave as shown in Fig. 5.

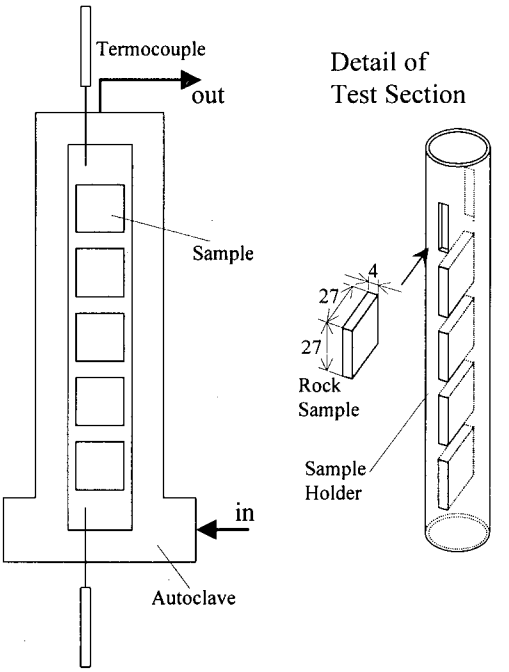

Fig. 5 One-through autoclave. Five rock specimens are set in the holder.

The major difference between this autoclave and the batch autoclave is that fresh water is continuously supplied to the autoclave by a high pressure pump. The experimental conditions are the same as previous section, that is, temperatures are 200 °C, 250 °C, 300 °C, 330 °C and 350 °C and the pressure is 18 MPa. The water flow rate was 1.0×10^{-2} m^3/h, sufficient to keep the "granite" concentration in the water to a very low value. The weight losses of the specimens were calculated in the same way as described in the previous section. Fig. 6 summarizes the results of these experiments for each temperature and run time.

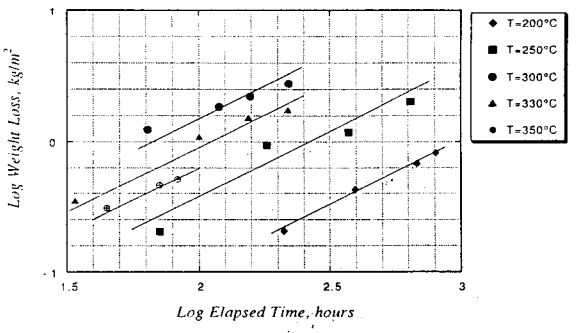

Fig. 6 The weight loss of rock specimens. Solid lines are the best fit lines when the reaction rate is assumed to be constant during experiments.

The reaction rate must change somewhat with time, because of the changes of reaction condition, such as total area of reaction surface. In this study, however, we assumed that the reaction rate did not change with time and that the weight losses should be proportional to the run time. Based on this assumption, straight line fits were obtained as shown in Fig. 6. These lines show the rate of weight loss with time.

In these experiments, the amount of fresh water being supplied continuously into the autoclave is large enough to assume that the concentration in the autoclave is almost equal to zero. Therefore, equation 1 can be eritten as :

$$\frac{\partial C}{\partial t} = \frac{S}{\rho_W \cdot Q} \cdot K(T) \cdot C^{\infty}(T) \qquad (8)$$

The weigh loss per unit area, ΔW can be calculated by following equation, according to mass balance.

$$\Delta W = \Delta C \cdot \rho_W \cdot Q / S \qquad (9)$$

Therefore :

$$\frac{\partial W}{\partial t} = \frac{\rho_W \cdot Q}{S} \cdot \frac{\partial C}{\partial t} = K(T) \cdot C^{\infty}(T) \qquad (10)$$

The left side of equation 10 is the rate of weight loss which we have measured by these experiments. The solubility of granite, $C^{\infty}(T)$, was measured in previous section. Therefore, the dissolution rate constant, $K(T)$, can be calculated based on equation 10. Fig. 7 shows $K(T)$ for each temperature, and the fitting curve in Fig. 7 is used for the following numerical analysis.

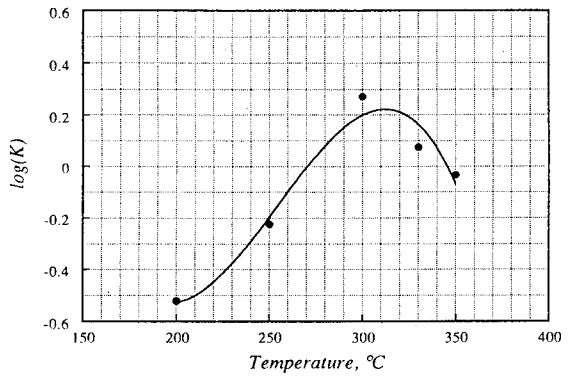

Fig. 7 The relationship between the dissolution rate constant and temperature. Solid curve is used for the numerical analysis.

ANALYSIS OF FRACTURE APERTURE CHANGE

In order to estimate the changes of the fracture apertures in geothermal reservoirs, the one-dimensional water flow model as shown in Fig. 8 has been introduced. In this model, it is assumed that the injection water is saturated with rock and rock precipitation occurs instantaneously when the concentration exceeds the solubility.

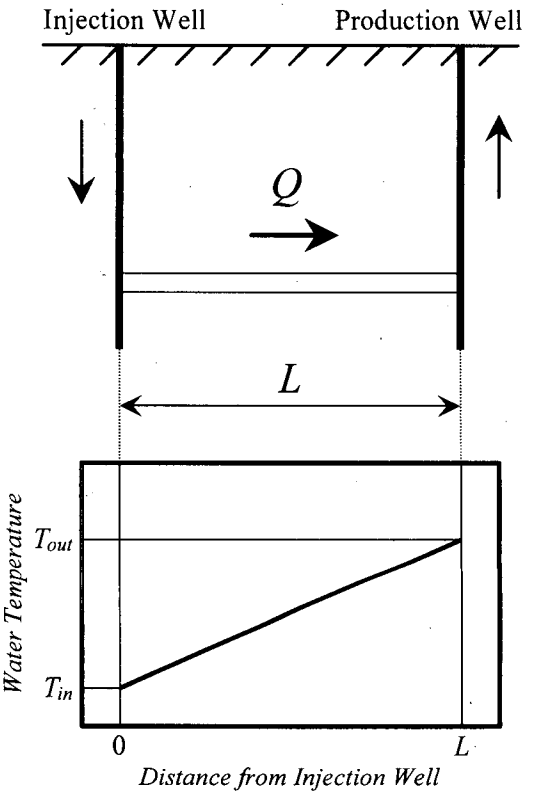

Fig. 8 A model of one-dimensional water flow through a fracture. The water temperature increases linearly with the distance from the Injection well.

In this model, water flow occurs only through the parallel-sided fracture, and the water temperature increases linearly through the fracture as shown also in Fig. 8. The water temperature at inlet and outlet are expressed by T_{in} and T_{out} respectively. The distance between the injection well and the production well was set to be 200 m. Four examples with different condition as follows have been examined.

Ex. 1 : T_{in}=200 °C, T_{out}=300 °C, Q=10 m^2/h
Ex. 2 : T_{in}=250 °C, T_{out}=350 °C, Q=10 m^2/h
Ex. 3 : T_{in}=200 °C, T_{out}=300 °C, Q=100 m^2/h
Ex. 4 : T_{in}=250 °C, T_{out}=350 °C, Q=100 m^2/h

The analytical result of the concentration change through the fracture for the Ex. 1 is shown by solid line in Fig. 9 (a). The dashed line expresses the saturation solubility at each point, i. e., each temperature along the fracture. Fig. 9 (b) shows the changes of fracture aperture after 2, 4, 6, 8 and 10 years. The corresponding results for Ex. 2, Ex. 3 and Ex. 4 are shown in Fig. 10, Fig. 11, and Fig. 12 respectively.

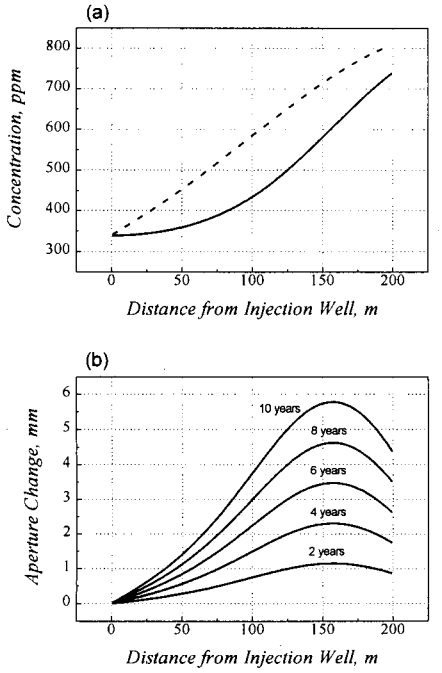

Fig. 9 The change of concentration and fracture aperture along the fracture for Ex. 1. The concentration never reached saturation, therefore, precipitation did not occur at any point.

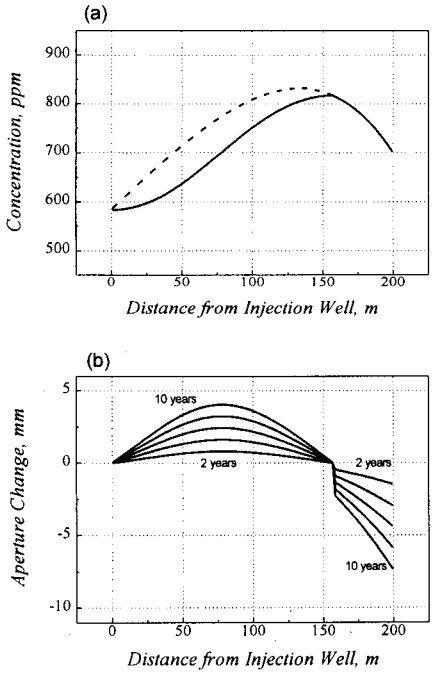

Fig. 10 The change of concentration and fracture aperture along the fracture for Ex. 2. The concentration reached saturation, and precipitation occurred at certain point.

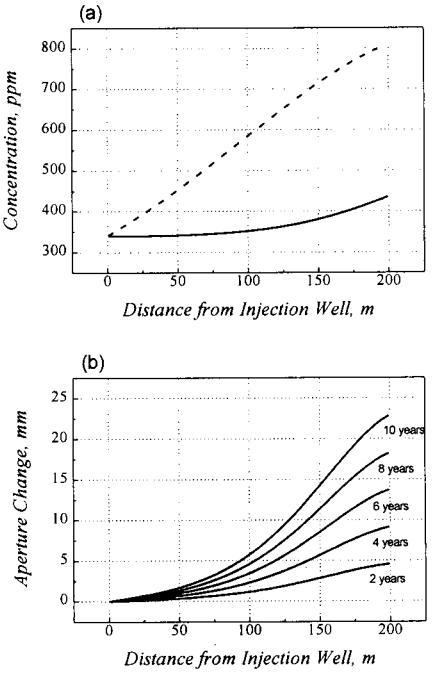

Fig. 11 The change of concentration and fracture aperture along the fracture for Ex. 3. The water flux is fast enough not to make a large change in the concentration.

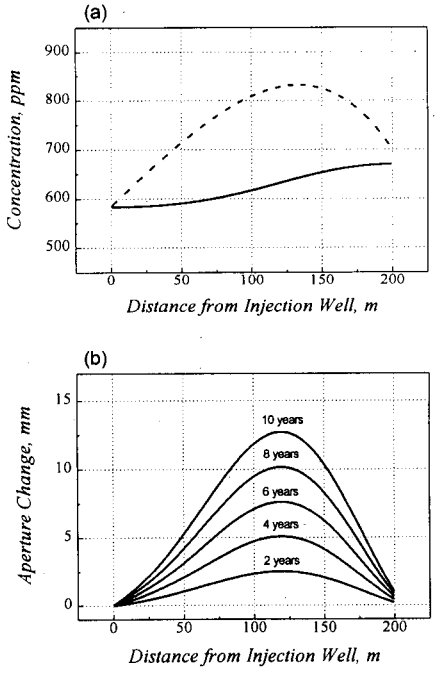

Fig. 12 The change of concentration and fracture aperture along the fracture for Ex. 4. The water flux is fast enough to prevent the precipitation.

In Ex. 1, the solubility increases along the fracture and the concentration never reached the solubility. This allowed only dissolution and results in widening the fracture aperture. In Ex. 2, on the other hand, the concentration reached saturation and precipitation occurred from this point. The water flux used for Ex. 3 and Ex. 4, Q=100 m^2/h, is large enough to prevent the concentration along the fracture increasing significantly. Even in Ex. 4, where temperature condition was same as Ex. 2, precipitation did not occur at any point.

COMPARISON WITH EXPERIMENTAL DATA

To help verify the numerical results, we have developed the tube-reactor type autoclave as shown in Fig. 13. This autoclave makes it possible to simulate water flow in a fracture using cylindrical rock specimens. Five separate heaters are attached along the 1 m long tube, and several kind of temperature gradient can be set. In order to examine the precipitation behavior suggested in the previous section, the experimental temperate was selected to be around 320 °C. Two experiments with different water flow rate (0.5 mm^3/s and 5 mm^3/s) were performed. The number of cylindrical specimens used for each run was 50. The water temperatures were set 250 °C, 300 °C, 330 °C, 350 °C and 340 °C at each heater point from the inlet. The last heater was set lower to prevent the output water boiling.

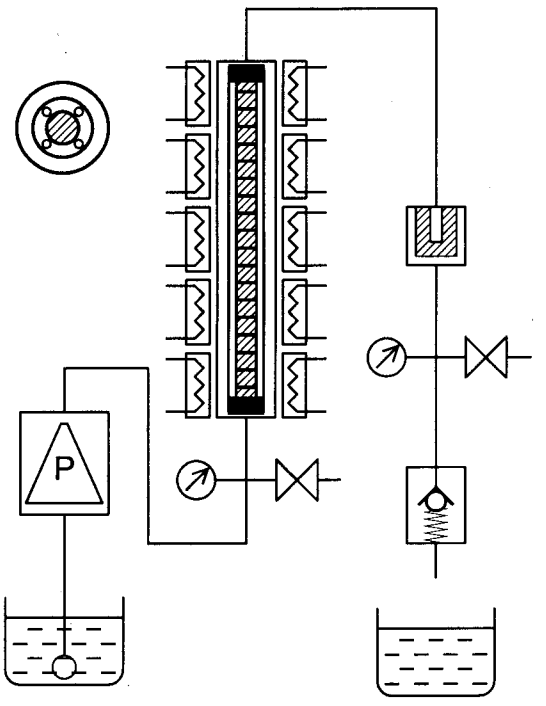

Fig. 13 Tube-reactor autoclave. Temperature gradient can be introduced along the flow path using five heaters.

Figure 14 (a) shows the weight changes of the specimens along flow path measured from the experiment with Q=0.5 mm^3/s. The weight of some specimens increased due to precipitation. This lappened at the point where the temperature exceeded 320 °C, as same as the numerical analysis. Fig. 14 (b) shows the concentration profile calculated from weight loss of specimens, and the solid line is the solubility of granite for each point. A region of over-saturation was found. This means that the precipitation rate constant should be also considered in order to inprove the numerical model presented here.

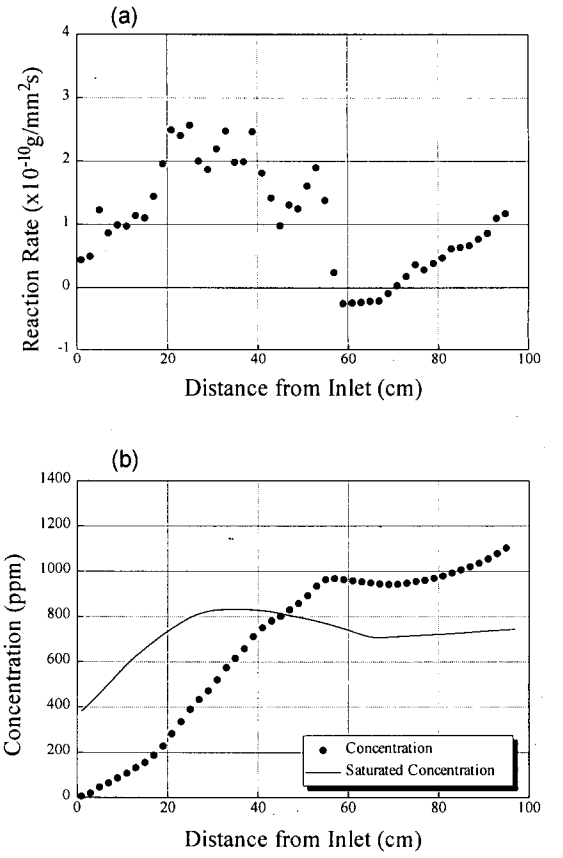

Fig. 14 The reaction rate and the calculated concentration along flow path obtained from the experiment for Q=0.5 mm^3/s. Rock precipitation occurred around the point of 60 cm from inlet. The water was over saturated from the point of 45 cm from inlet.

Figure 15 shows the results for the experiment with Q=5 mm^3/s. In this experiment, no specimen increases its weight and the concentration never reached asturation. However, the dissolution rate decreased from the point where temperature exceeded 320 °C.

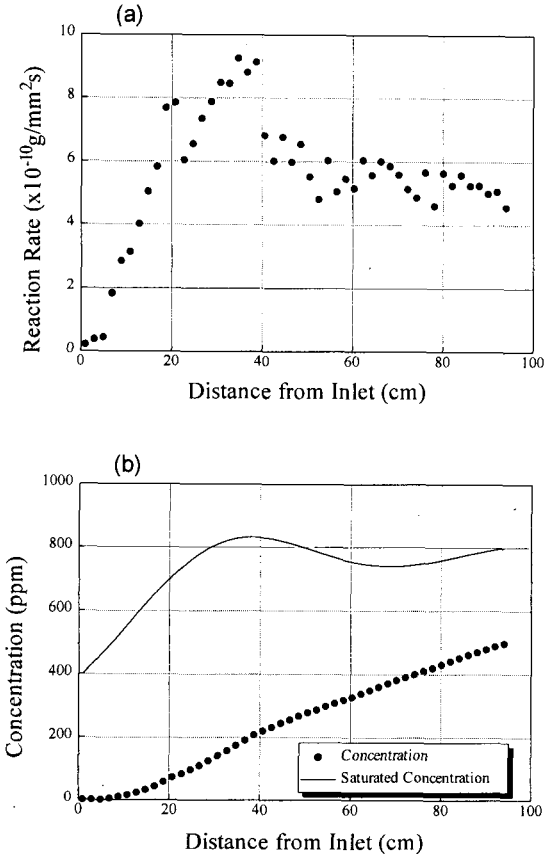

Fig. 15 The reaction rate and the calculated concentration along flow path obtained from the experiment for Q=5.0 mm^3/s. Water flux was sufficiently high that the saturation concentration was never reached, and no precipitation could not take place.

CONCLUSIONS

The solubility of granite may be dominated by quartz, and its sensitivity to temperature was similar to that of quartz. Fractures in geothermal reservoirs may be subjected to various chemical problems depending on temperature, flow rate and other parameters. The analytical and experimental results in this study suggest that rock precipitation can occur and may result in the plugging of the fractures in geothermal energy extraction systems whose reservoir temperatures exceed 300 °C.

Although, in this study, precipitation was assumed to occur at the point where the concentration exceeds the solubility, experimental results suggest that rock supersaturation persist for some time. This implies that the precipitation rate constant should also be measured in future work.

ACKNOWLEDGMENT

A part of this work presented here was supported by Ministry of Education, Science and Culture under Grant-in-Aid for Scientific Research on Priority Areas entitled "Fractal Fracture Mechanics and Advanced Geothermal Energy Extraction System Design," Grant No. 05232101, 05232102 and 05232104.

REFERENCES

Hashida, T. and Takahashi, H. (1983) "Dissolution Behavior of Granite under Simulated Geothermal Reservoir Conditions," 4th International Symposium Water-Rock Interaction, Extended Abstracts, pp. 172-174.

Kennedy, G. C. (1950) "A Portion of the System Silica-Water," Econ. Geol. Vol. 45, pp. 629-253.

Kitahara, S. (1960) "The Solubility of Quartz in Water at High Temperatures and High Pressures," The Review of Physical Chemistry of Japan, Vol. 30-2.

Rimsted, J. D. and Barnes, H. L. (1980) "The Kinetics of Silica-Water Reaction," Geochimica et Cosmochimica Acta, Vol. 44, pp. 1683-1699.

Robinson, B. A. and Pendergrass, J. (1989) "A Combined Heat Transfer and Quartz Dissolution/Deposition Model for A Hot Dry Rock Geothermal Reservoir," Proceeding of 14th Workshop on Geothermal Reservoir Engineering, Stanford University.

Takahashi, H. and Hashida, T. (1992) "New Project for Hot Wet Rock Geothermal Reservoir Design Concept," Proceedings of the 17th Workshop on Geothermal Reservoir Engineering, Stanford University, Vol. 17, pp. 39-44 (SGP-TR-141).

Tester, J. W., Brown, D. W. and Potter, R. M. (1989) "Hot Dry Rock Geothermal Energy - A New Energy Agenda for the 21st Century," Los Alamos National Laboratory report LA-11514-MS.